PERGAMON

Journal of Structural Geology 22 (2000) 947–967

JOURNAL OF STRUCTURAL GEOLOGY

www.elsevier.nl/locate/jstrugeo

Matrix mosaics, brittle deformation, and elongate porphyroclasts: granulite facies microstructures in the Striding–Athabasca mylonite zone, western Canada

Simon Hanmer

Geological Survey of Canada, 601 Booth St, Ottawa, Ontario, Canada, K1A 0E8

Received 5 May 1998; accepted 21 December 1999

Abstract

The Late Archean Striding–Athabasca mylonite zone, western Canadian Shield, is a 400-km-long, linked system of granulite facies mylonite belts developed in the continental crust. The granulite facies mylonites (800–1000°C at 0.8–1.1 GPa) developed in subsets of the anhydrous mineral assemblage clinopyroxene–orthopyroxene–garnet–plagioclase–quartz ± hornblende. Comparison of the microstructures of the Striding–Athabasca mylonites with published descriptions of natural and experimental deformation of geological and analogue materials at elevated homologous temperatures provides some insight into the role played by different processes in the development of the Striding–Athabasca mylonites.

In addition to dislocation creep and dynamic recrystallisation, extensive mass transfer occurred contemporaneously with brittle fracture and cataclasis during granulite facies metamorphism. The microstructure and extreme phase dispersal in anhydrous polymineralic matrix mosaics is indicative of efficient grain-scale and aggregate-scale diffusion, grain boundary mobility, and mass transfer, at relatively slow strain rates. Despite their annealed appearance, the granoblastic matrix mosaics developed synkinematically; deformation-induced dilation may enhance metamorphic reactions where products are more voluminous than reactants. In the porphyroclast population, highly elongate (> 20:1) monocrystalline orthopyroxenes appear to be fragments of dismembered, kinked parent grains, rather than stretched porphyroclasts.

Granulite facies mylonites should not be treated as direct analogues of greenschist facies mylonites. In particular, it is essential to evaluate the potential positive feedback between structural and metamorphic processes in highly strained, high-temperature shear zone rocks.

1. Introduction

Geologists working with deformed rocks are generally aware of the structures and processes involved in the formation of mylonites at low to moderate temperatures, typical of the greenschist to lower amphibolite facies (e.g. Bell and Etheridge, 1973; Knipe, 1989). Even non-specialists are familiar with grain size reduction by dynamic recrystallisation, porphyroclasts vs. matrix grains, ribbon grains, *S–C* and core-and-mantle microstructures. However, high temperature mylonites formed at upper amphibolite to granulite facies commonly have a very different microstructural aspect. They may be granoblastic and relatively coarse grained, and preferred grain shape orientation fabrics can be weakly developed to absent. It is commonly difficult to discriminate between synkinematic and static post-kinematic microstructure, and to recognise the mylonites for what they are: highly strained shear zone rocks. Examples include the upper amphibolite facies Central Metasedimentary Belt boundary thrust zone, Grenville Orogen, Ontario (Hanmer, 1988; Hanmer and McEachern, 1992), and the granulite facies Striding–Athabasca mylonite zone, northern Saskatchewan (Hanmer et al., 1994, 1995a,b; Hanmer, 1997). In both, mylonites were previously identified as successions of thinly bedded, moderately deformed, supra-

E-mail address: shanmer@nrcan.gc.ca (S. Hanmer).

0191-8141/00/$ - see front matter
PII: S0191-8141(00)00009-2

crustal rocks, but are now known to represent exhumed, deep-seated, crustal-scale shear zones.

This paper describes and illustrates three characteristic features of the granulite facies microstructure developed in the Striding–Athabasca mylonite zone: (i) the development of polymineralic matrix mosaics, and the dispersion of mineral phases within them, (ii) brittle fracture and microcataclasis, and (iii) the formation of extremely elongate porphyroclasts. These features were selected, either because they do not occur in low temperature mylonites, or because geologists do not generally associate them with deformation at very high temperatures. Comparisons are then made with published descriptions of natural and experimental deformation of geological and analogue materials at elevated homologous temperatures, in an attempt to identify the panoply of processes, which probably operated in the Striding–Athabasca mylonites. One of the principal conclusions of this study is that the microstructure of the Striding–Athabasca mylonites was strongly influenced by extensive grain-scale and aggregate-scale mass transfer, and contemporaneous cataclasis, in addition to dislocation creep. Furthermore, it is suggested that granulite facies mylonites should not be treated as direct analogues of greenschist facies mylonites.

The microstructural observations presented here are principally optical, supported by scanning electron microscope (SEM) images and microprobe analyses obtained at the Electron Microscopy Laboratory, Geological Survey of Canada. Detailed petrofabric observations made on the Striding–Athabasca mylonites have been presented elsewhere (Ji et al., 1993). Because the three categories of microstructure examined here are so different from one another, the description of each is immediately followed by the relevant Discussion section. A synthesis of the deductions and inferences drawn for the Striding–Athabasca mylonites as a whole is presented in Section 4 at the end of the paper.

2. Striding–Athabasca mylonite zone

The Late Archean (ca. 2.6 Ga) Striding–Athabasca mylonite zone occupies a 400-km-long segment of the Snowbird tectonic zone in the western Canadian Shield (Fig. 1; Hanmer et al., 1994, 1995a,b; Hanmer, 1997). It is a geometrically complex, linked system of granulite facies mylonite belts that formed under conditions in the range 800–1000°C, at 0.8–1.1 GPa (Snoeyenbos et al., 1995; Williams et al., 1999). The Striding–Athabasca mylonite zone consists of two parts: the East Athabasca mylonite triangle, and its northeastern extension, the Striding mylonite belt. Only a brief geological overview of the mylonite zone is presented here; detailed descriptions of the field relations are given in the above-cited publications, to which the interested reader is referred.

The East Athabasca mylonite triangle (Fig. 1; Hanmer, 1994) is structurally divided into an upper and a lower deck (Hanmer et al., 1994). The lower deck consists of three kinematic sectors, comprising two conjugate, penetratively mylonitic, strike-slip shear zones, each about 15 km thick, separated by a central septum. Mylonite development in the central septum is less penetrative than in the flanking shear zones, and the widespread presence of small-scale conjugate shear zones is indicative of progressive pure shear (Hanmer et al., 1994; Hanmer, 1997). The upper deck structurally overlies the lower deck and was initially emplaced along a discrete basal thrust, as indicated by the presence of relict, very high pressure assemblages in the hanging wall (Snoeyenbos et al., 1995). It is now entirely occupied by a penetratively mylonitic, 10-km-thick, dip-slip shear zone. To the northeast, the Striding mylonite belt is a sinuous, 5–10-km-thick corridor of ribbon mylonites (Hanmer et al., 1995a) that crosses the Saskatchewan territorial border. Extension lineations throughout the Striding–Athabasca mylonite zone plunge shallowly to the southwest, and the overall kinematic framework is one of strongly transpressive, dextral strike-slip shearing (Hanmer et al., 1995b).

3. Mylonite microstructure

Macroscopically, the Striding–Athabasca mylonites are uniformly fine-grained rocks, with or without obvious ribbon structure or compositional lamination. Locally, they can be traced with continuity into coarse-grained granitic, noritic, gabbroic or migmatitic protoliths (see Hanmer et al., 1994, 1995a,b, and Hanmer, 1997, for detailed macroscopic and field observations). The scarcity of preserved feldspar porphyroclasts has been attributed to an elevated recrystallisation rate/strain rate ratio, and the general participation of all the quartzo-feldspathic component of the rock in the imposed bulk deformation (Hanmer et al., 1995b; Williams et al., 1999; see also Hanmer, 1987). Microscopically, most of the mylonites consist of a fine grained (ca. 100 μm) polycrystalline quartzo-feldspathic or feldspathic mosaic, with variable proportions of pyroxene, garnet, hornblende ± feldspar porphyroclasts. The following observations were made on thin sections cut perpendicular to the mylonitic foliation and parallel to the extension lineation. Boundaries separating grains of the same mineral will be referred to as grain boundaries, whereas those separating grains of different minerals will be called phase boundaries (e.g. Means and Park, 1994).

3.1. Matrix mosaics

In rocks of the Striding–Athabasca mylonite zone, the polycrystalline mylonite matrix mosaic is commonly compositionally layered on a ca. 0.5–1 mm scale. Individual layers may be monomineralic (quartz, clinopyroxene, or single feldspar), or polymineralic combinations of two feldspars, pyroxenes, hornblende, garnet and quartz. Although they commonly extend beyond the dimensions of the thin section, most layers are laterally discontinuous and lenticular. Monomineralic, polycrystalline layers may contain relict porphyroclasts in core-and-mantle structures, suggesting that the layers were directly derived by grain-size refinement.

In general, the microstructure of the polycrystalline mosaics in the Striding–Athabasca mylonites is statistically homogeneous from the centimetre to the outcrop scale. A first type of matrix is composed of highly strained 100–500 μm grains with undulatory extinction indicative of strong lattice distortion, separated from one another by narrow zones, or a more or less extensive matrix mosaic of small (10–50 μm), internally strained, inequigranular new grains. This is well shown by feldspar, where the gradation between optical subgrains and new grains of similar dimensions suggests a rotational component to the process of dynamic recrystallisation (White, 1976; Urai et al., 1986), and relict porphyroclasts deform by kinking, or internal boudinage (Cobbold et al., 1971).

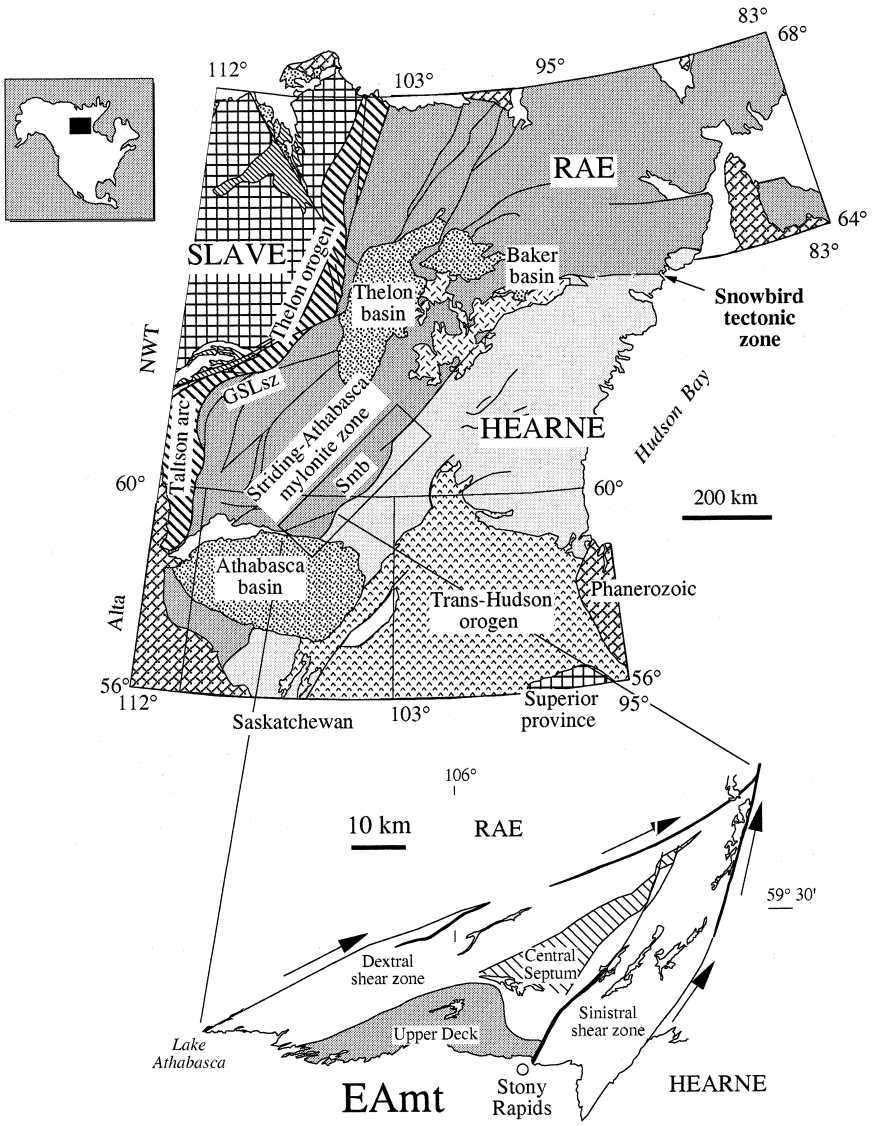

Fig. 1. Schematic map of the tectonic setting of the Striding–Athabasca mylonite zone, northwest Canadian Shield. EAmt: East Athabasca mylonite triangle. Smb: Striding mylonite belt. GSLsz: Great Slave Lake shear zone. Rae and Hearne are domains of the Western Churchill structural province.

Fig. 2. Reticular matrix mosaic. Grain boundary network of a coarser subaggregate of antiperthite grains forms a reticular or cross-hatched pattern. Long side of photo is 2.8 mm. Crossed polars.

A second type of matrix has an optically relaxed[1] microstructure composed of moderately strained to strain-free, equigranular grains (100–500 μm). They show mildly undulose or patchy extinction, with irregular, commonly lobate grain boundaries and triple junctions of unspecified geometry (Fig. 2). The grains commonly have a square or diamond shape, forming a reticular or cross-hatched pattern. A finer (50 μm) population of grains (subaggregate), up to an order of magnitude smaller than the first, and locally of different composition, commonly decorates the grain boundary network of the coarser subaggregate (Fig. 3). Compositional changes include plagioclase decorated by a finer, more sodic feldspar subaggregate (over the range Ab 40–50 mol.%), or antiperthite decorated by polycrystalline plagioclase. In places, this bimodal microstructure is preserved as the intermediate stage between large monocrystalline porphyroclasts and a uniform, fine grained matrix mosaic, and grains in both subaggregates may be internally strained. Taken together, these observations suggest that the microstructure is the product of dynamic recrystallisation, rather than post-kinematic annealing.

[1] *'Relaxed'* is used to describe a microstructural state intermediate between strongly strained and statically annealed. Use of the term implies that stored strain energy, present as dislocations in the crystal lattice and a potential driving force for grain boundary migration, has been relieved by recovery and/or recrystallisation, while recognising that the surface energy of the grain boundary network is greater than that of an equivalent annealed microstructure (e.g. Urai et al., 1986).

3.1.1. Discussion

Similar aggregates with reticular grain shapes and bimodal grain size have been attributed to grain boundary sliding, associated with grain boundary diffusion and highly mobile grain boundaries (e.g. Lister and Dornsiepen, 1982; Gapais and Barbarin, 1986; Drury and Humphreys, 1988; Tullis, 1990; Herwegh and Handy, 1996). Aggregates with bimodal grain size and subaggregates of different compositions have been experimentally produced in two stages by cataclasis and sintering (Tullis and Yund, 1992). However, similar microstructures in deformed ice and other analogue materials have been attributed to dynamic recrystallisation related to the heterogeneity of strain in grain margins undergoing active dislocation creep (Wilson, 1986; Herwegh and Handy, 1996).

In naturally deformed rocks and experimentally deformed analogue materials, reticular or cross-hatched grain shape patterns have been variously attributed to (i) close crystallographic control over highly mobile grain boundaries, indicative of high temperatures (Gapais and Barbarin, 1986), (ii) growth-related alignment of the grain boundaries with directions of elevated resolved shear stress (Boland and Tullis, 1986), and (iii) grain boundary sliding, coupled with extensive grain boundary migration, diffusive mass transfer and grain boundary pinning by second phase particles or impurities (Lister and Dornsiepen, 1982; Lister and Snoke, 1984; Herwegh and Handy, 1996). Experimental deformation of geological materials has shown that square-cornered forms, similar to those in reticular grain shape patterns, are favoured by grain boundary sliding, associated with relatively slow strain

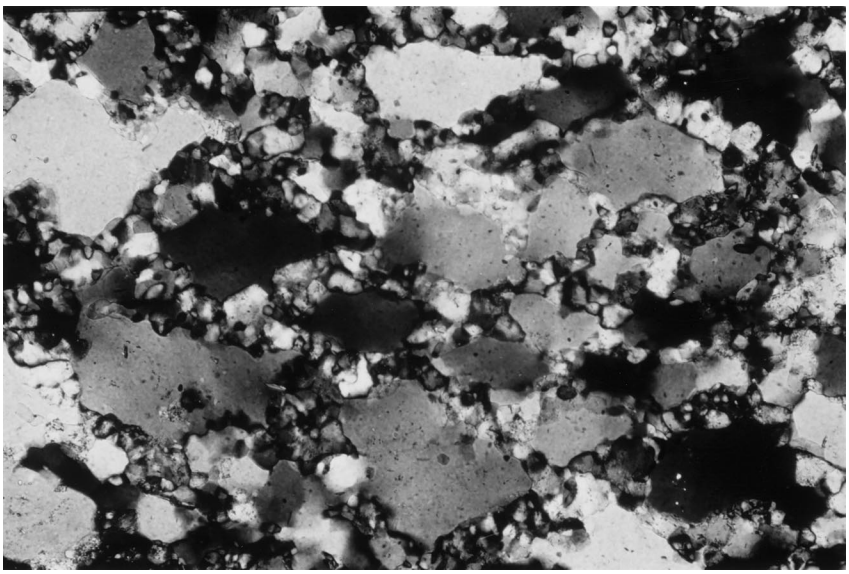

Fig. 3. Reticular matrix mosaic with bimodal grain-size distribution, where the coarser K-feldspar subaggregate is decorated by a finer grained population of plagioclase grains. Long side of photo is 2.8 mm. Crossed polars.

rates, high temperatures, enhanced grain growth, and grain boundary diffusion creep (Drury and Humphreys, 1988; Tullis, 1990, figures 6e and 8; Tullis and Yund, 1991; see also Herwegh and Handy, 1996). In the granulite facies Striding–Athabasca mylonites, such conditions would reflect the high temperatures of deformation recovered from these rocks (Snoeyenbos et al., 1995; Williams et al., 1999). From the foregoing discussion, the observed microstructures are suggestive of relatively slow strain rates, and highly mobile grain boundaries.

In many mosaics of the Striding–Athabasca mylonites, the finer subaggregate is also compositionally distinct from the coarser matrix grains (Fig. 3; see also Hanmer, 1982; Tullis and Yund, 1992). This implies that mass transfer to and/or along the grain boundary network occurred during their formation (Tullis and Yund, 1991), despite the dry nature of the mineral assemblage. The nature of diffusion paths in deforming high temperature aggregates is a complex issue (e.g. Elliot, 1973; Yund and Tullis, 1980; Yund et al., 1981, 1989; White and Mawer, 1986; Beeman and Kohlstedt, 1993; Farver and Yund, 1995; Yund, 1997). However, theoretical and experimental considerations notwithstanding, work on natural materials suggests (i) that a hydrous fluid is essential for effective grain boundary diffusion (Florence and Spear, 1995), and (ii) that grain boundary diffusion will dominate in any aggregate-scale diffusive process (Farver and Yund, 1996). In summary, it would appear that the reticular, bimodal matrix mosaics of the Striding–Athabasca mylonites are indicative of efficient *grain-scale diffusion* and highly mobile grain boundaries, and associated grain boundary sliding.

3.2. Phase dispersion

A third type of matrix comprises a granoblastic microstructure composed of optically strain-free, equigranular (100–250 μm), polygonal grains, with straight boundaries of uniform length, and evenly spaced 120° triple junctions. In polymineralic layers, phase boundaries are strongly favoured over grain boundaries (Fig. 4). In quartzo-feldspathic rocks, this may be expressed as the dispersion of small (10–50 μm), round quartz grains located preferentially at triple junctions in the plagioclase grain boundary network (cf. figure 6 in Hanmer, 1982, and figure 2 in Hanmer, 1984). The development of dispersed quartz grains in the microstructure is commonly accompanied by a reduction in the continuity of monomineralic quartz ribbons, and their increasingly corroded aspect. In mafic, polymineralic compositions, irregularly shaped vermicular, hook- or shard-like orthopyroxene grains are dispersed along the grain boundary network of a granoblastic plagioclase mosaic (Fig. 5). The shapes of the orthopyroxene grains, only slightly smaller than the polygonal plagioclase grains, reflect their growth along the grain boundary network of the matrix mosaic. Associated coronitic microstructures indicate that orthopyroxene and plagioclase are the products of reactions consuming garnet and clinopyroxene (Fig. 6). Although the matrix mosaics have a granoblastic appearance (Figs. 4 and 5), vermicular orthopyroxene–plagioclase symplectite in strain shadows on garnet indicates that these reactions were synkinematic (Fig. 6; Brodie, 1995).

Within polyphase matrix mosaics, rotation of the microscope stage commonly reveals the existence of

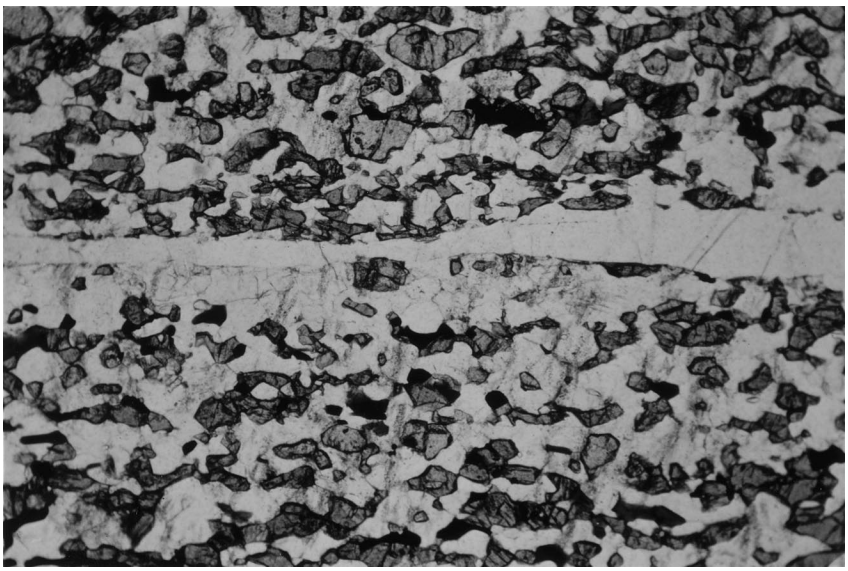

Fig. 4. Vermicular orthopyroxene and clinopyroxene, plus anhedral garnet, are dispersed along the grain boundary network of a granoblastic, polycrystalline plagioclase matrix mosaic. Note the strain-free, equigranular, equant polygonal grains with straight boundaries of uniform length and evenly spaced 120° triple junctions. The quartz layer cutting across the middle field is parallel to the regional foliation. Long side of photo is 2.8 mm. Plane polarised light.

orientation families (Urai, 1983; Urai et al., 1986), where several seemingly separate neighbouring grains pass in and out of extinction together. This feature is best developed in orthopyroxene set in a granoblastic plagioclase matrix (see Fig. 5).

3.2.1. Discussion

The granoblastic aspect of the microstructure does not necessarily constitute prima facie evidence for post-kinematic annealing. Dynamic microstructure may not register, let alone preserve, the complete strain history of a deforming rock. For example, a balance between processes that enhance shape fabrics, and those that weaken them, can result in strain-insensitive, or steady-state foliation, which only records the later increments of the deformation (Means, 1981; Hanmer, 1984). Where grain boundaries are sufficiently mobile, a strain-free microstructure involving delicate crystal shapes may predominate during progressive deformation, and the flowing aggregate may not develop

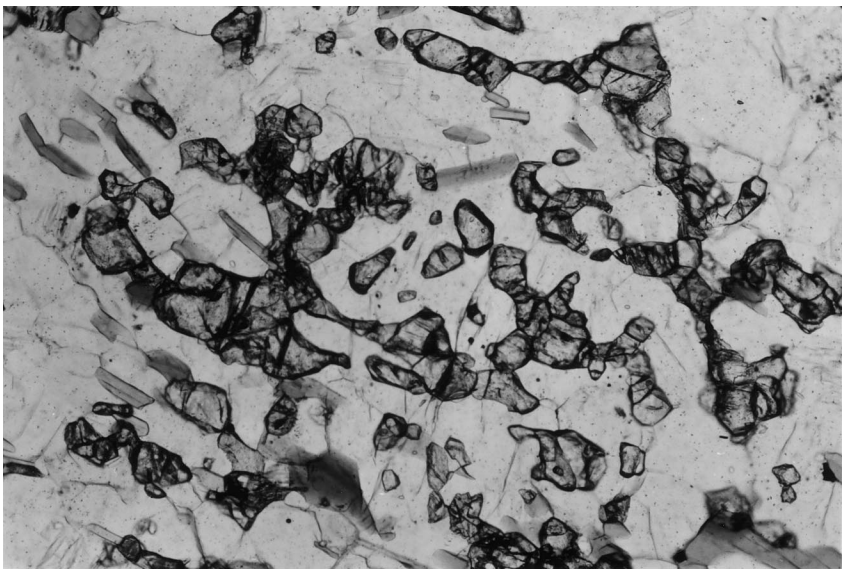

Fig. 5. Vermicular orthopyroxene (high relief) dispersed along the grain boundary network of a polycrystalline plagioclase matrix mosaic. Note the equigranular, equant polygonal grains (low relief) with straight boundaries of uniform length and evenly spaced 120° triple junctions. Some of the orthopyroxene components in this image are part of an extinction family. Long side of photo is 1.1 mm. Plane polarised light.

any shape fabric at all, as has been demonstrated in deformation experiments on analogue materials (Means and Park, 1994; Park and Means, 1996).

Some workers have attributed dispersion of mineral phases in polymineralic mosaics to an essentially mechanical process of grain boundary sliding and nearest neighbour switching during deformation ('superplastic' behaviour; e.g. Gueguen and Boullier, 1974; Boullier and Gueguen, 1975; Kerrich et al., 1980). Other workers have associated it with neocrystallisation of new grains by heterogeneous classical nucleation, due to chemical disequilibrium (e.g. Fitz Gerald and Stunitz, 1993; Stunitz, 1998; Kruse and Stunitz, 1999; Newman et al., 1999). Yet other researchers have interpreted phase dispersion in terms of the enhancement of phase boundaries at the expense of grain boundaries, by a decrease in the surface energy of the aggregate, in materials as diverse as undeformed granites, metasediments, and granulite facies gneisses (Flinn, 1969; Vernon, 1974, pp. 135–147; Hickey and Bell, 1996). It has been suggested that this process might also operate in mylonites (Hanmer, 1984; Bell and Johnson, 1989). Such a model requires optimum conditions for *aggregate-scale diffusion*, such as elevated diffusion rates, minimal activation energy barriers, and short diffusion paths, much as would pertain in hot, fine-grained mylonites (Hanmer, 1984).

Surface energy considerations for phase dispersal apply in both static and dynamic environments. Indeed, interfacial energy is more likely to be the determining factor if the constituent grains of the aggregate are *not* deforming internally (Hickey and Bell, 1996), although this does not require static conditions (e.g. Means and Park, 1994). On the other hand, in the Striding–Athabasca mylonites, orthopyroxene dispersed throughout the plagioclase mosaics is the product of the reaction garnet–clinopyroxene → orthopyroxene–plagioclase (Fig. 5). This reaction, which also produced well-preserved, orthopyroxene–plagioclase symplectites in strain shadows on garnet (Fig. 6), is synkinematic. Most importantly, it implies a positive volume change of the order of 12–17% (Brodie, 1995). Given the pressures recovered from these rocks (ca. 1.0 GPa), the reaction would have been enhanced in an environment where void space was being dynamically created (Brodie, 1981). Microscopically, such sites can be generated during grain boundary sliding (e.g. Zhang et al., 1994b), at pull-apart interfaces, or at strain incompatibilities between neighbouring grains of variable stiffness in a deforming viscous aggregate (e.g. Wilson, 1986; Zhang et al., 1994a; see also Rutter and Brodie, 1992). Dilational voids have been observed in the grain boundary networks of deforming polycrystalline mosaics of analogue materials (Urai, 1983; Means, 1989; see also Zhang et al., 1994a), as well as some natural examples (Behrmann and Mainprice, 1987). They could provide sites for the products of the metamorphic reaction (e.g. Kruse and Stunitz, 1999), and result in the kind of polymineralic matrix described here (see Figs. 4 and 5). Accordingly, the dispersed, granoblastic, mosaic microstructure of the Striding–Athabasca mylonites might plausibly result from a dynamic combination of phase boundary enhancement associated with neocrystallisation, *plus* flow-induced grain boundary dilation during a metamorphic reaction where the products occupy more volume than the reactants.

Orientation families in the dispersed polyphase

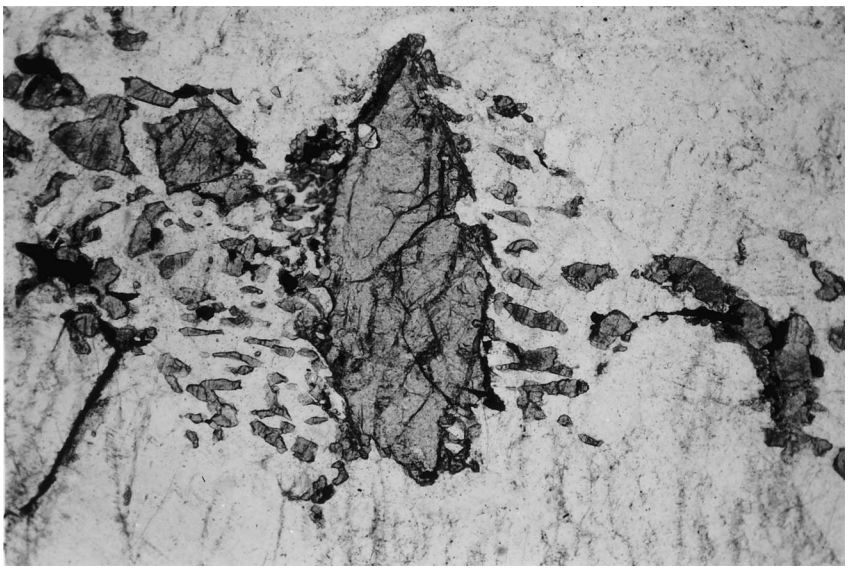

Fig. 6. Garnet grain (dark grey) in plagioclase matrix, with synkinematic vermicular orthopyroxene (light grey) and plagioclase developed in the strain shadows. Foliation trace (not visible) is horizontal. Long side of photo is 1.1 mm. Plane polarised light.

mosaics may point to grain mobility during the development of the Striding–Athabasca mylonites. On the one hand, it is possible that they represent the intersections of the branches of individual skeletal or dendritic grains with the plane of the thin section. Such spongiform grains could grow post-kinematically. On the other hand, in experiments with actively deforming analogue materials, orientation families are seen to form where diffusive mass transfer is very efficient, and grain boundaries are highly mobile. Grains in deforming aggregates are seen to migrate as material entering through the leading edge of the grain boundary is balanced by material leaving via the trailing edge (e.g. Urai et al., 1986; Means, 1989; Bons and Urai, 1992). Synkinematic grain migration ('micromotion' of Means, 1983) results in mutual dissection of grains as they pass through one another, producing 'families' comprising isolated volumes with the same crystallographic orientation (Means and Dong, 1982; Means, 1983; Urai, 1983; Urai et al., 1986). Only rarely have similar microstructural processes been inferred in natural examples (Lafrance et al., 1996), but the presence of orientation families, the elevated metamorphic temperatures, and other microstructural indications of highly mobile grain boundaries, allow the possibility that dynamic grain migration could have occurred in the Striding–Athabasca mylonites.

3.3. Microcataclasis

In the Striding–Athabasca mylonites, clinopyroxene commonly forms discrete, continuous, parallel-sided polycrystalline layers, about 1 mm thick (Fig. 7). The origin of the polycrystalline microstructure is equivocal. In some cases, fine-grained mosaics of clinopyroxene are spatially associated with larger, internally kinked grains, and evidence of bulge nucleation and migration of the kink band boundaries is locally preserved. Alternatively, there is a progression from polycrystalline clinopyroxene, via a clinopyroxene mosaic with isolated, round to vermicular plagioclase grains dispersed along the grain boundary network, to a clinopyroxene–plagioclase aggregate with a high proportion of phase boundaries, compared to grain boundaries. In some examples, the plagioclase is visibly located along brittle fractures that divide the initially coarse grained clinopyroxene layer into square or diamond-shaped grains (Fig. 8). However, other clinopyroxene layers show a microstructural spectrum ranging from closely packed, equigranular, equant fragments of clinopyroxene (Fig. 9), to angular, irregularly shaped fragments of a range of sizes, all set in an ultra-fine-grained granular matrix of clinopyroxene with minor amphibole. Locally, fractures cut the clinopyroxene matrix and bound thin monocrystalline slices of clinopyroxene excised from initially coarse parent grains (Fig. 10). SEM images of clinopyroxene $\pm$ plagioclase aggregates show that relatively large (50 μm) clinopyroxene grains are bounded by complex domains composed of angular fragments of clinopyroxene, separated by thin films or irregularly shaped fields of hornblende and opaque oxides (Fig. 11a). The hornblende shapes include right-angle bends and triangular volumes (r and t, respectively, in Fig. 11a). Some of the hornblende fields contain isolated angular fragments of clinopyroxene, and the angular shapes of the

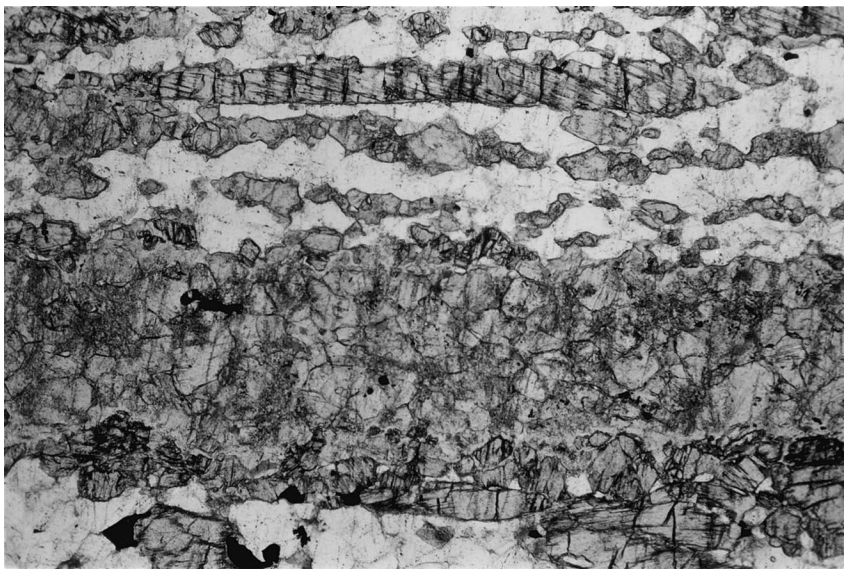

Fig. 7. Elongate orthopyroxene grain with oblique (100) cleavage set in a matrix of polycrystalline plagioclase (top). The polycrystalline layer below it is clinopyroxene with a rim of polycrystalline orthopyroxene and garnet along its lower side. Long side of photo is 2.8 mm. Plane polarised light.

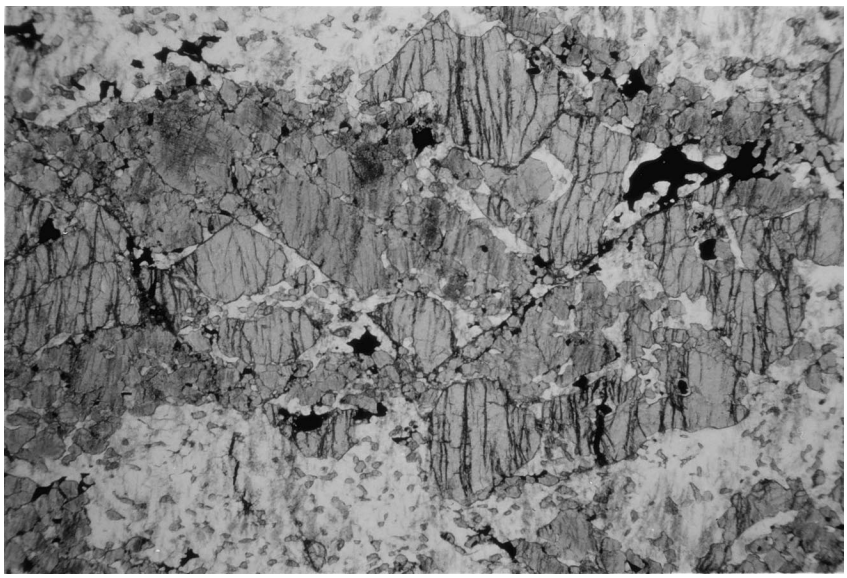

Fig. 8. Clinopyroxene–garnet–plagioclase aggregate where the plagioclase is located along brittle fractures that divide the initially very coarse-grained clinopyroxene layer into square or diamond-shaped grains. The garnet grains can be distinguished by their vertical internal fracture arrays. Long side of photo is 2.8 mm. Plane polarised light.

amphibole fields resemble dilated fractures. For the most part, there is no significant change in the hedenbergitic clinopyroxene composition with grain size. However, in some samples, the smaller grains are more calcareous, and have lower Fe/Mg ratio, and lower Al_2O_3 and TiO_2 contents than the coarser ones. Boundaries between clinopyroxene grains may show a progression from trains of very small (1 μm), apparently unconnected, plagioclase grains ± hornblende, via narrow, irregular shaped channels of plagioclase, to large (< 50 μm) plagioclase fields with ragged margins (Fig. 11b and c). Promontories and inclusions of clinopyroxene within the plagioclase are extremely angular (Fig. 11c) and have the appearance of fracture-delimited fragments. Taken together, these observations appear to track the progressive dilation of complex microfractures in the clinopyroxene, accompanied by limited replacement by hornblende and the introduction of plagioclase, at fracture controlled sites. The presence of continuous, non-fractured, garnet coronas around pervasively fractured clinopyroxene, even where interstitial hornblende is present, shows that the fracturing is not a post-granulite, retrograde microstructure.

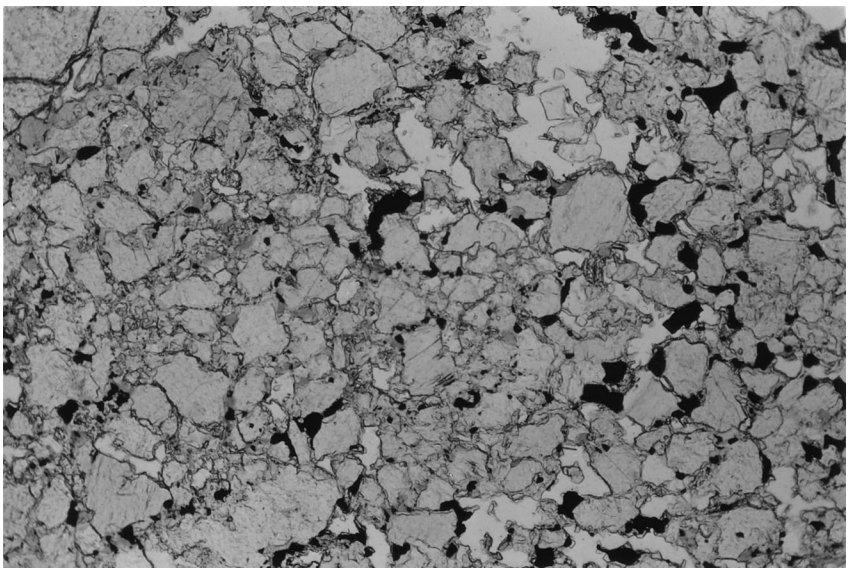

Fig. 9. Closely packed, equigranular, equant fragments of clinopyroxene. Note the irregular shapes of the fragments and the fine-grained matrix between them. Long side of photo is 1.1 mm. Plane polarised light.

3.3.1. Discussion

The commonly used microstructural criteria for cataclasis include variable grain size and angular grain shape (Stel, 1981; Nyman and Tracy, 1993; Lafrance and Vernon, 1993), plus the presence of obvious fractures and sites of dilation, all of which are observed in the Striding–Athabasca mylonites on a variety of microscopic scales. The microstructure and mineralogy illustrated in Figs. 9 and 11 resemble a fine grained aggregate described by Brodie (1981), who attributed the presence and location of a new, less dense phase between denser, older grains to metamorphic reaction during cataclastically induced dilation. In addition, the presence of plagioclase at dilatant sites within cataclastically deformed clinopyroxene layers (Fig. 7) lends support to the suggestion that the reaction garnet–clinopyroxene → orthopyroxene–plagioclase, which requires a volume increase, is enhanced by deformation-induced dilation (see Section 3.2.1).

3.4. Brittle fracture and mass transfer

The Striding–Athabasca mylonites commonly contain monomineralic quartz layers. The most highly attenuated and laterally continuous examples are typical quartz ribbons (Boullier and Bouchez, 1978), whereas others are morphologically more complex, comprising branching and anastomosing strands of variable thickness. Many quartz layers are intermediate in character and could be termed 'branching ribbons'. However, the geometry of such layers suggests that they are not derived by the intracrystalline deformation of individual parent grains (cf. Mackinnon et al., 1997). In addition, they commonly contain discontinuous, wall-parallel septa or trails of feldspar, pyroxene, garnet or amphibole. Most trails are asymmetrically disposed about the centre line of the quartz layer. In many cases, individual trails can be traced back to an angular step in the layer boundary (Fig. 12). Successive steps commonly show the same sense of offset, and pyroxene and garnet grains in the walls are locally truncated against the quartz layers. This morphology suggests that the layers grew both longitudinally and laterally by the precipitation of quartz in propagating and dilating stepped fracture arrays (Mackinnon et al., 1997 and references therein). In other words, these quartz 'ribbons' are veinlets.

Elongate, rectangular grains of garnet, with aspect ratios up to 10:1, and shard-like clinopyroxene grains, lie along and parallel to the boundaries of the quartz veinlets (Fig. 13). The lengths of the elongate garnet grains are comparable with the widths of equant or euhedral garnet elsewhere in the same sections, suggesting that the rectangular grains are fracture delimited slabs. The brittle deformational behaviour of garnet in the continental crust is well documented (e.g. Gregg, 1978; Williams and Compagnoni, 1983; Carney et al., 1991), although some authors interpret elongate garnet as the product of crystal plasticity (Ji and Martignole, 1994; challenged by den Brok and Kruhl, 1996).

Clinopyroxene tails, or strain-shadows, commonly occur on the ends of the garnet slabs (Fig. 13). Similar concordant, rectangular, garnet grains, with clinopyroxene, also occur discontinuously inside the quartz layers. If the garnet and clinopyroxene have the same

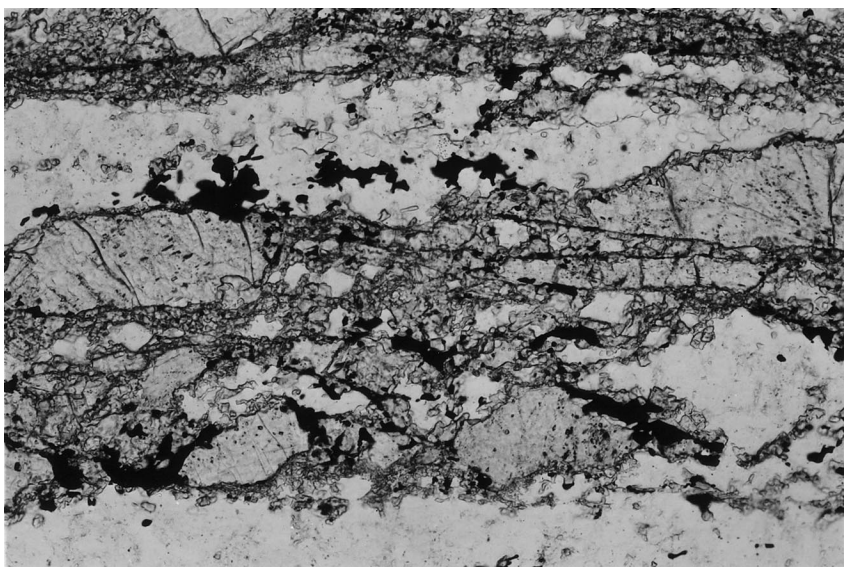

Fig. 10. Clinopyroxene layer (medium grey) bound by plagioclase layers. Large rectangular grains of clinopyroxene are delimited by discrete brittle fractures. The spatially associated very fine-grained material is mostly clinopyroxene, with traces of hornblende (not visible). Long side of photo 1.1 mm. Plane polarised light.

origin as their equivalents along the quartz layer boundaries then, in the absence of similar fractions of feldspar inclusions, they appear to imply that the lateral growth of the quartz veinlets involved a component of volume replacement of the wall material.

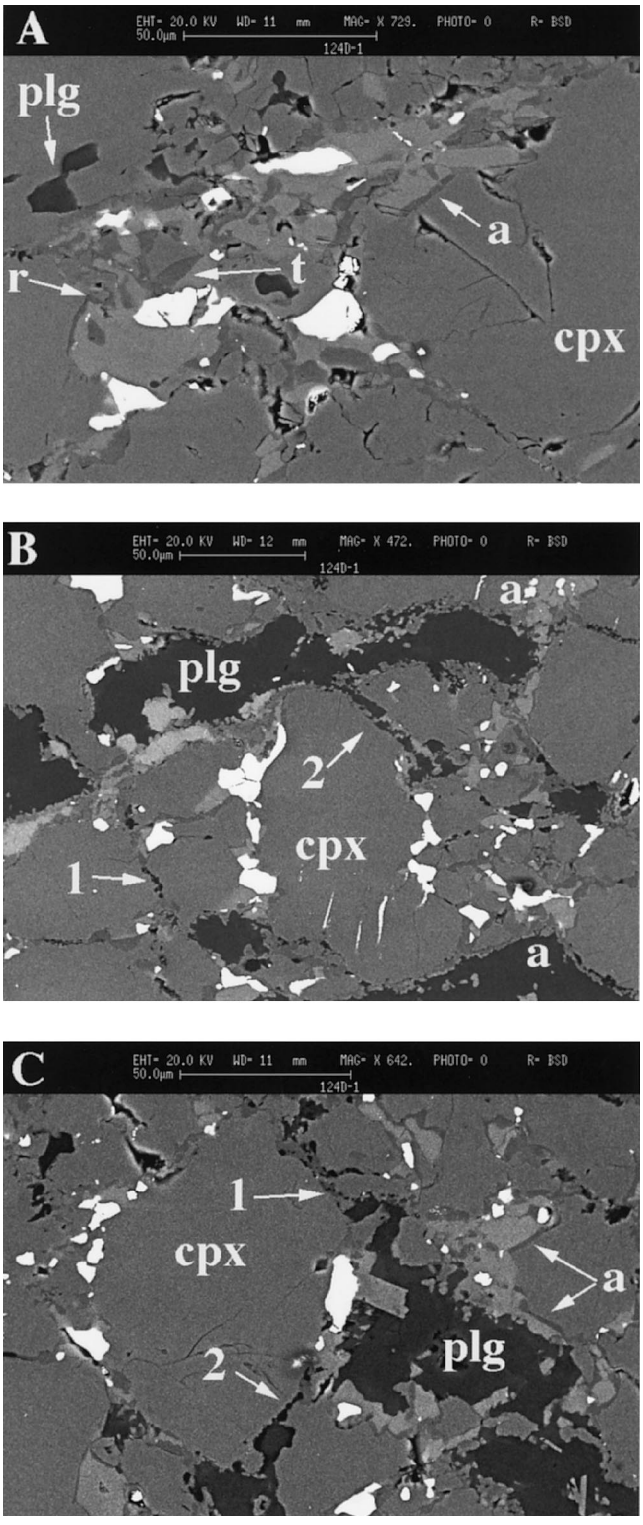

Fig. 11.–(*continued opposite*).

3.4.1. Discussion

Ribbon-like quartz layers decorated with garnet slabs and angular clinopyroxene fragments are further evidence that fracture and dilation occurred at granulite facies. The introduction of quartz fill along the fracture arrays, and the spatially associated presence of clinopyroxene strain shadows on garnet, also require that mass transfer was able to operate effectively at this metamorphic grade. In light of the conclusion by Florence and Spear (1995) that a hydrous phase is essential for effective grain boundary diffusion, plus the local development of minor hornblende in clinopyroxene microcataclasite (Fig. 11), 'water' must have been present during deformation in the Striding–Athabasca mylonites, if only transiently. Not only would a hydrous phase enhance diffusion, but it could also mechanically promote fracturing and cataclasis if it were present as a fluid (e.g. Etheridge, 1983; Etheridge et al., 1983, 1984; Rutter and Brodie, 1988, 1992). Although not described in this contribution, the extensive development of synkinematic anatexis (see Hanmer, 1994, 1997; Hanmer et al., 1994, 1995a) is compatible with the presence of 'water' at elevated temperatures in these rocks.

3.5. Elongate porphyroclasts

Elongate single grains of plagioclase and orthopyroxene occur with aspect ratios commonly up to 20:1, and more. They are up to two orders of magnitude larger than the grains of the matrix mosaics and are consistently aligned in the mylonite foliation. Similar structures have been referred to as 'tabular' porphyroclasts, or 'ribbon grains' by other authors (e.g. Mercier and Nicolas, 1975; Bouchez, 1977).

3.5.1. Plagioclase

The elongate plagioclase grains (An 60) are usually set within a fine grained (50–100 µm) feldspar mosaic of similar composition, with which they show a pro-

Fig. 11. Backscattered electron SEM images of microstructure in clinopyroxene. (A) Large clinopyroxene grains (cpx) adjacent to aggregate of angular fragments of clinopyroxene, with thin (dark grey) films (a) or irregular shaped fields of hornblende (r and t), and opaque oxides (white). (B) Progressive development of large plagioclase fields with ragged margins (plg) from trains of plagioclase grains (1), via narrow, irregular shaped channels (2). The preservation of microstructure identical to '1' is visible to the right of 'a' (lower right). Note the irregular shapes of the hornblende in the aggregate (a–a), very similar to A. (C) A large plagioclase field (plg) with ragged margins, a very angular clinopyroxene promontory (right of central opaque grain), and inclusions of clinopyroxene. The plagioclase field is bounded by clinopyroxene aggregate with hornblende (a), similar to A and B. Plagioclase develops at clinopyroxene grain boundaries by a similar progression (1 and 2) to that seen in (B).

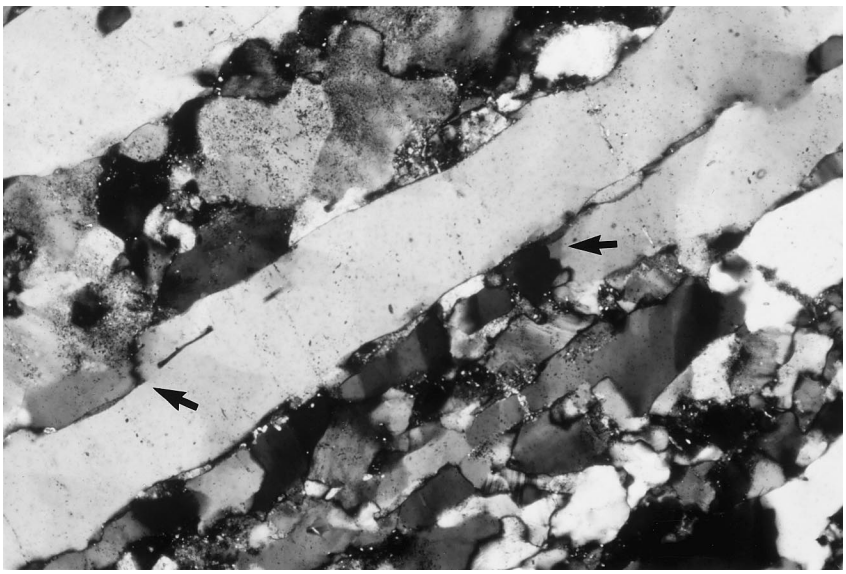

Fig. 12. Ribbon-like aspect of quartz layers. Note the angular steps (arrows) in the boundaries of the quartz layer (light grey) and the septa of feldspar, which extend into the quartz from the step. Long side of photo is 1.1 mm. Crossed polars.

gressive boundary, associated with optical subgrains of similar size to the matrix grains (Fig. 14). Locally, they are bent around stubby plagioclase porphyroclasts. Where present, (010) twins make a low angle (ca. 10°) with the long dimension of the elongate grain (Fig. 14). Untwinned elongate grains are commonly crossed at a high angle by regularly spaced, oblique subgrain walls. In some cases, a well-defined outer limit to the surrounding monomineralic plagioclase mosaic indicates the form and volume of the original parent grain, and demonstrates that the elongate plagioclase is part of a core-and-mantle structure (Fig. 14). In other cases, the volume of the mantle mosaic represents a small proportion of the core-and-mantle structure. Either the rate at which new grains were fed into the mantle was low compared with the strain rate, and the mantle mosaic has flowed away from the core (cf. Passchier and Simpson, 1986), or the plagioclase core was already elongate prior to the formation of the mantle. In the latter case, the elongate form could be the result of intracrystalline deformation. However, where the elongate grain represents a relatively small volume compared with the enclosing plagioclase mosaic, its shape may be a consequence of the distri-

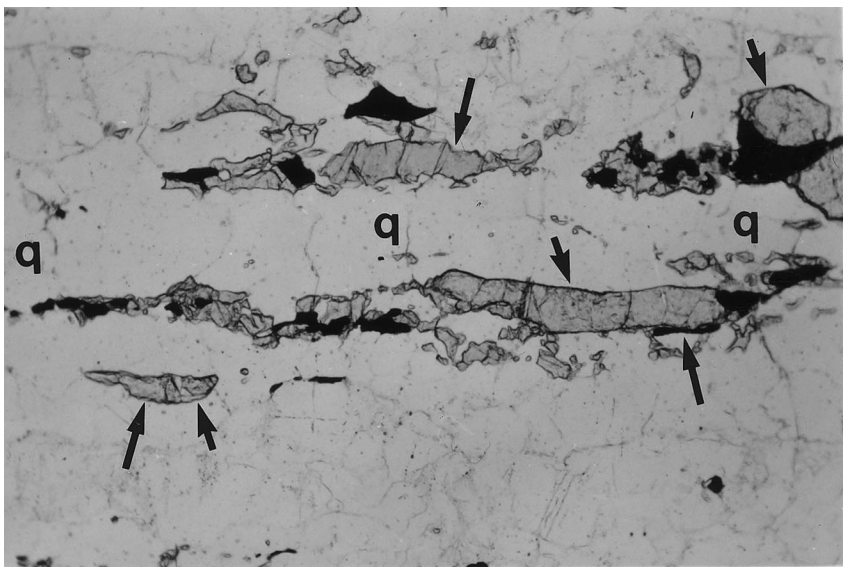

Fig. 13. Elongate, rectangular grains of garnet (long arrows) and shard-like clinopyroxene grains (short arrows) lie along and parallel to the boundaries of a quartz layer (q). Clinopyroxene tails on the ends of the garnet grains are taken as evidence for mass transfer processes in a nominally anhydrous assemblage. Long side of photo is 1.1 mm. Plane polarised light.

Fig. 14. (010) Twins make a low angle (ca. 10°) with the long dimension of an elongate plagioclase grain set in a polycrystalline plagioclase mosaic. A well-defined outer limit to the surrounding monomineralic plagioclase mosaic (boundary between monomineralic and polyphase mosaics) indicates the form and volume of the parent grain and demonstrates that the elongate plagioclase is part of a core-and-mantle structure. Long side of photo is 2.8 mm. Crossed polars.

bution of recrystallisation in a parent grain of unknown size and form. In this case the shape of the elongate grain, or porphyroclast, would bear no first-order relationship to the magnitude of the bulk strain experienced by the rock (e.g. Olesen, 1987).

3.5.2. Orthopyroxene

Although in some respects the elongate orthopyroxene grains are morphologically similar to the plagioclase examples, it is the differences that are highlighted here. The orthopyroxene is uniformly aluminous and enstatitic (En75). Aspect ratios tend to be higher for orthopyroxene than for plagioclase (Fig. 15). Elongate orthopyroxene grains commonly occur in close proximity to coarse, stubby crystals of the same composition, and are commonly deformed around them. The (100) cleavage is almost always visible in thin section and invariably lies at a low angle (ca. 10°) to the long dimension of the elongate grain (Figs. 7 and 15). In samples containing a statistically significant population of elongate orthopyroxene grains, the sense of internal obliquity of (100) may be symmetrically bimodal

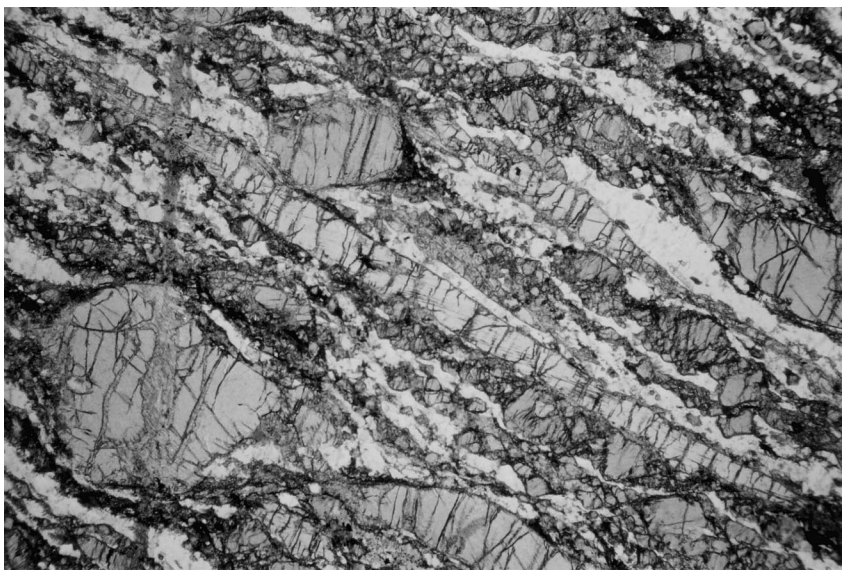

Fig. 15. Highly elongate and stubby orthopyroxene grains set in a matrix of fine grained polycrystalline orthopyroxene and plagioclase. Note the anticlockwise oblique (100) cleavage within the elongate orthopyroxene. Long side of photo is 7.5 mm. Plane polarised light.

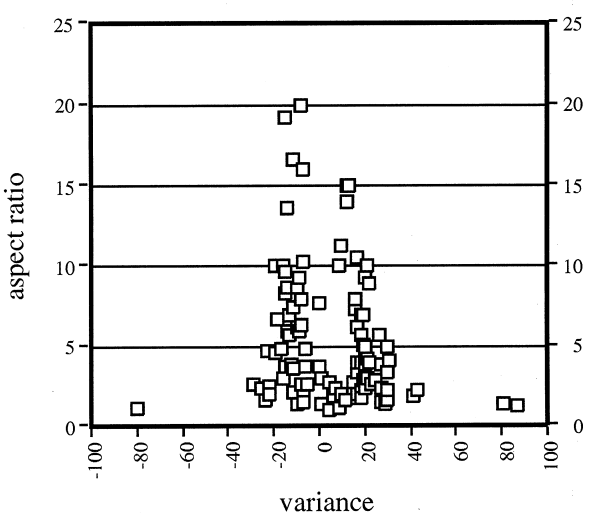

Fig. 16. Bimodal distribution of angles made with the matrix foliation and the long axis of the host grain by traces of the (100) cleavage in elongate orthopyroxene grains from a single thin section.

(Fig. 16). This microstructure resembles that observed in peridotites, where orthopyroxene is inferred to have undergone intracrystalline deformation by slip on (100)[001] (e.g. MacKenzie, 1960; Carter and Raleigh, 1969; Darot and Boudier, 1975; Tubia, 1994; Ross and Wilks, 1995; Brodie, 1995).

The setting of orthopyroxene within a core-and-mantle structure, or in a matrix mosaic, resembles the foregoing descriptions for plagioclase, with similar considerations regarding the origin of the aspect ratio of the elongate grains. However, in contrast to plagioclase, individual elongate orthopyroxene grains commonly occur completely surrounded by a second phase, e.g. plagioclase (Fig. 7). As before, their shape could be the result of intracrystalline deformation. However, some elongate grains set in a plagioclase matrix exhibit an irregular, delicately scalloped form along their long sides. This suggests that their shape has been modified to some degree by transverse phase boundary migration, involving either growth or corrosion of the orthopyroxene. In some examples, the shape variation of the elongate grains is coarse, even mimicking the morphology of a pinch-and-swell structure (Fig. 17). In such cases, the constant orientation of (100) throughout the grain, especially where coupled with abrupt changes in grain thickness, raises the possibility that the elongate shape of some orthopyroxene may not directly reflect intracrystalline strain. This suggestion derives further support from rather stubby, weakly deformed examples, which otherwise present all of the above features of their more highly elongate equivalents, including the obliquity of (100) with respect to the external foliation. However, the aspect ratios of the isolated elongate grains, and the orientation of their (100) cleavage, closely resemble individual high aspect ratio kink bands preserved in some large porphyroclasts (Fig. 18). In rare, well-preserved grains, alternating, high aspect ratio kinks are linked by box-fold closures (Fig. 19).

3.5.3. Discussion

Some authors have clearly demonstrated that elongate grains can be the product of intracrystalline deformation (Nicolas et al., 1973; Bouchez, 1977; Boullier and Bouchez, 1978; Weathers et al., 1979; Ji

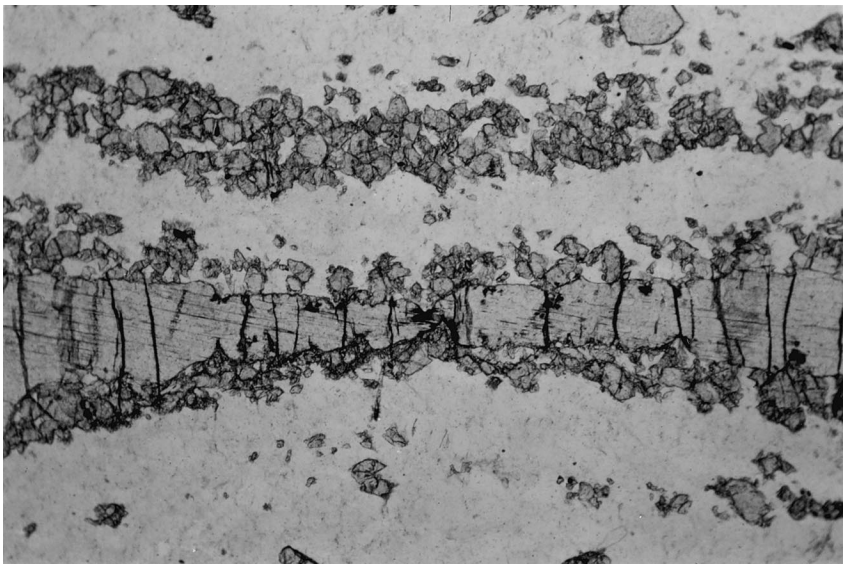

Fig. 17. Elongate orthopyroxene grain with oblique (100) cleavage set in a matrix of polycrystalline plagioclase. Thickness variation of the elongate grain mimics the morphology of a pinch-and-swell structure, but the (100) cleavage orientation remains constant throughout the grain. Long side of photo is 2.8 mm. Plane polarised light.

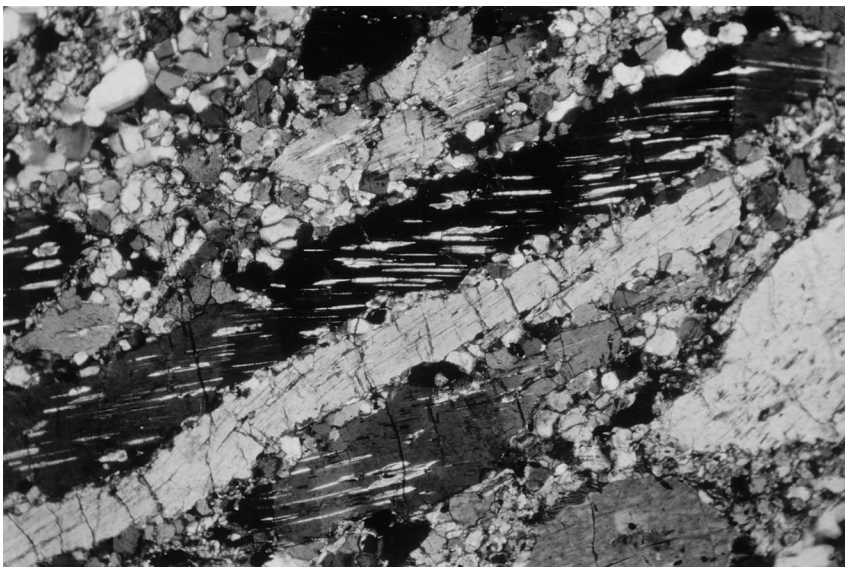

Fig. 18. Elongate orthopyroxene segment (light grey) with oblique (100) cleavage bounded on either side by two kinks of the same sign (black) and separated from them by kink band boundaries. Compare the light grey grain with Figs. 7 and 15. Crossed polars. Long side of photo is 2.8 mm.

et al., 1988). Extreme elongation of orthopyroxene, locally with highly strained inclusions (Goode, 1978), is commonly attributed to intracrystalline glide on single slip systems, possibly accommodated by Ca and Mg diffusion (Mercier, 1985). In the classical model, deformation occurs by slip on spinning (100) glide planes within the crystal lattice (Nicolas and Poirier, 1976; Etchecopar and Vasseur, 1987). Most workers note a systematic, asymmetrical low angle (ca. 5–10°) obliquity between the mineral cleavage and the crystal elongation, similar to that in the Striding–Athabasca mylonites (Figs. 7 and 20a). Alternatively, slip on initially non-spinning planes parallel to the bulk flow plane in the matrix has been invoked to account for oblique elongation of orthopyroxene (Fig. 20b; Goode, 1978). A symmetrically bimodal distribution of internal slip planes in elongate grains, similar to that in the Striding–Athabasca mylonites (Fig. 16), has been taken as indicative of bulk pure shear at the scale of the aggregate (Fig. 20c; Basu, 1977). However, from simple calculation, (e.g. Ramsay, 1967, p. 441), such highly elongate grains as occur in the Striding–Athabasca mylonites could not form from a stubby precursor purely by slip on (100), unless the slip planes were

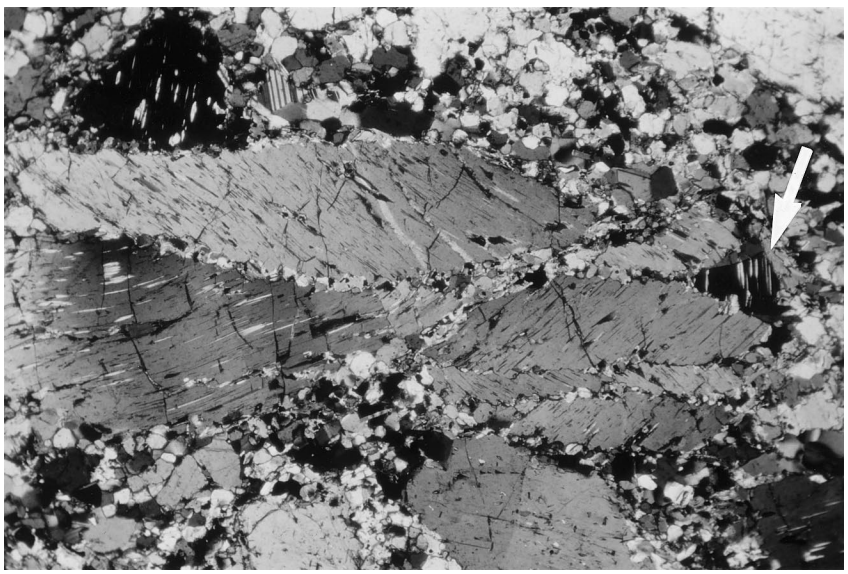

Fig. 19. Well-preserved orthopyroxene grain deformed by alternating kinks of high aspect ratio. Note the box-fold closure in extinction to the right (white arrow). Compare with Figs. 7, 15 and 18. Crossed polars. Long side of photo is 2.8 mm.

initially perpendicular to the present orientation of the long axis of the porphyroclast.

In short, it is possible to obtain the extreme elongation of orthopyroxene observed in the Striding–Athabasca mylonites by internal slip on (100), but only for grains with a special initial crystallographic orientation with respect to the principal axes of finite strain. Moreover, if they are the product of strain, the absence of dynamic recrystallisation in highly elongate porphyroclasts requires a very high degree of dislocation mobility, by either glide (e.g. Urai et al., 1986; Knipe and Law, 1987) or climb (e.g. White and Mawer, 1986, 1988). Although these rather specific conditions could be satisfied by the feldspars, it is unlikely that they could be met by orthopyroxene due to the extreme sluggishness of dislocation climb (Kohlstedt and Vander Sande, 1973; Etheridge, 1975, Nazé et al., 1987). The microstructural observations presented in this study suggest that there are alternatives.

Extreme intracrystalline flow is not the only deformation behaviour that can produce elongate grains. For example, they may result directly from the kinking of parent grains poorly oriented for slip (Fig. 21a). Kinks form readily in plagioclase and in pyroxene, in part because the rate of dislocation climb may be slow, and in part because of the well-developed rheological anisotropy conferred by lamellar twinning (Tullis, 1990). Recrystallisation along kink-band boundaries can isolate the relict monocrystalline limbs of the original kinks as part of a mortar structure (Fig. 21b; Etheridge, 1975; Basu, 1977; Goode, 1978; Olesen, 1987; Ji and Mainprice, 1988; Bell and Johnson, 1989; Mawer and Fitz Gerald, 1993; Ross and Wilks, 1995). Alternatively, if kinks lock up, localisation of slip along the kink-band boundaries can slice the original grain into slabs, which are then isolated from one another by continued flow in the surrounding plagioclase matrix (see Figs. 7 and 21c; Ross et al., 1980).

The kink model would appear to explain satisfactorily most of the principal features of the highly elongate orthopyroxene grains, and some plagioclase porphyroclasts, in the Striding–Athabasca mylonites. In a symmetrical chevron fold variant, this model can

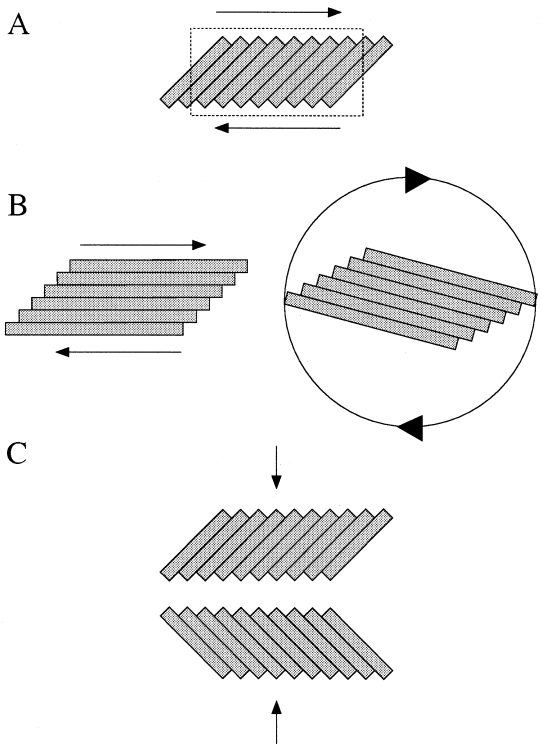

Fig. 20. Schematic illustrations of model interpretations for the obliquity of the (100) cleavage in elongate orthopyroxene grains. (A) Bookshelf-model. (B) Slip on initially non-spinning planes parallel to the bulk flow plane in the matrix results in oblique elongation of orthopyroxene. Rotation of the elongate grain in the matrix flow (arrowed circle) results in rigid body rotation of the internal slip planes with respect to the bulk flow plane. (C) Bimodal distribution of internal slip planes in elongate grains may be indicative of bulk pure shear (shortening indicated) at the scale of the aggregate.

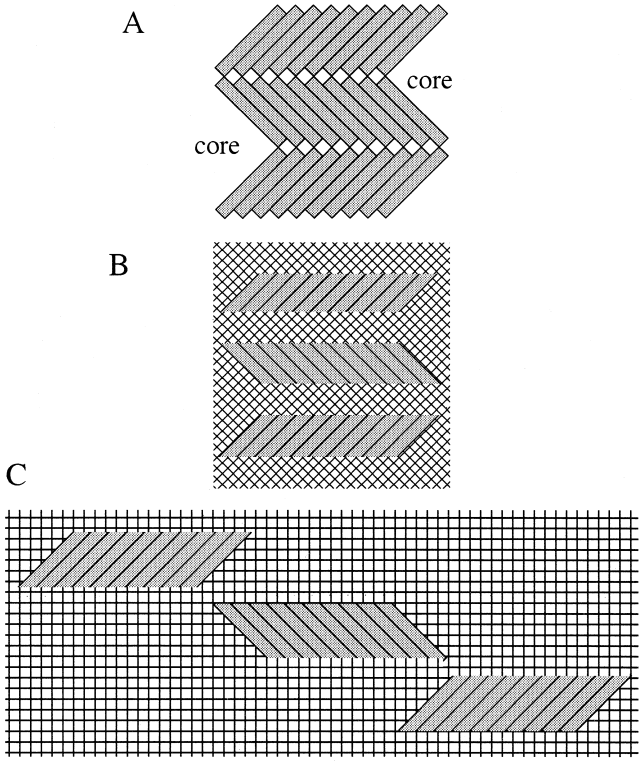

Fig. 21. Schematic illustrations of possible derivations of elongate grains with oblique internal cleavage from larger kinked parent grains (A). In (B), recrystallisation localised along the kink band boundaries produces relict elongate grains set in a polycrystalline mosaic of the same phase (diamonds). In C, the elongate grains are set in a second phase matrix (squares). When kinks in the old grain lock up, localisation of slip along the kink band boundaries leads to dismemberment of the parent grain, separation of the kinks and their isolation in a polycrystalline mosaic of unspecified composition (Ross et al., 1980).

also account for the locally conjugate orientations of the slip planes (Fig. 16). Recrystallisation of kinks can result in relict grains set in a mosaic of new grains of similar composition. However, a locked kink model (Ross et al., 1980), with dismemberment of folded porphyroclasts by slip along the kink band boundaries, appears to offer an elegant explanation for elongate grains isolated in a second phase matrix (Fig. 7). Subsequent intracrystalline slip along (100) is then required to reduce the angle made by the internal slip planes and the long axis of the porphyroclast from the locking angle inherent to the folding mechanism (ca. 30°; Ramsay, 1967), to the observed angle (ca. 10°). Nevertheless, the model should not be applied indiscriminately, because it is clear that not all elongate, monocrystalline cores represent low strain relict grains (e.g. Boullier and Bouchez, 1978; Goode, 1978; Brunel, 1980; Kohlstedt and Weathers, 1980).

4. Summary

Microstructures similar to those presented in this paper have been discussed and interpreted by other workers, who have deduced or inferred the processes that control their development. However, those studies have mainly focused on the deformational behaviour of individual minerals (e.g. Boland and Tullis, 1986; Nazé et al., 1987; Tullis and Yund, 1991, 1992; Beeman and Kohlstedt, 1993), or on the experimental deformation of natural or analogue materials (e.g. Urai, 1983; Wilson, 1986; Means, 1989; Tullis, 1990; Herwegh and Handy, 1996). Studies which address natural high temperature deformation of rocks have mostly been concerned with mantle materials (e.g. Gueguen and Boullier, 1974; Darot and Boudier, 1975; Mercier and Nicolas, 1975; Basu, 1977), or subsolidus magmas (e.g. Gapais and Barbarin, 1986). The present contribution has examined selected aspects of microstructural development in polyphase, polycrystalline aggregates in a natural, high temperature, regional-scale shear zone developed in continental crust.

For more than 20 years, the concept evolved that mylonites form by dislocation creep and dynamic recrystallisation of rock-forming minerals, leading to grain-size refinement (e.g. Bell and Etheridge, 1973; White, 1976; White et al., 1980; Urai et al., 1986; Hirth and Tullis, 1992) and the development of ribbons (Boullier and Bouchez, 1978). However, the granulite facies microstructure of the Striding–Athabasca mylonites appears to be the product of a more complex panoply of processes (see also Stunitz, 1998; Kruse and Stunitz, 1999; Newman et al., 1999). The presence of crystallographic preferred orientations in plagioclase and quartz in the Striding–Athabasca mylonites has been taken to indicate the operation of dislocation creep in those phases (Ji et al., 1993), and the presence of rare feldspar porphyroclasts testifies to the existence of initially coarse grain sizes, and to significant grain-size reduction. However, comparison of other facets of the Striding–Athabasca mylonites with published studies on naturally deformed mantle rocks and subsolidus magmas, and experimental deformation of natural and analogue materials, indicates that dislocation creep and dynamic recrystallisation only account for part of the microstructural development. The major role that other processes appear to have played in these hot, nominally dry rocks was unanticipated at the beginning of this study. Extensive grain boundary mobility, grain boundary diffusion and aggregate-scale mass transfer are indicated by the microstructure of the matrix mosaics, as well as the quartz veinlets and spatially associated clinopyroxene pressure shadows on elongate garnet fragments. The common occurrence of reticular grain boundary networks in the matrix mosaics, while commonly taken to indicate a component of grain boundary sliding, is also suggestive of elevated grain boundary mobility, accompanied by relatively slow strain rates. The important role of cataclasis and brittle fracture is highlighted by observations on both the matrix mosaics, and the quartz veinlets and associated garnet fragments. This was particularly unexpected, given the elevated temperatures recorded from these rocks, and the observational evidence favouring relatively slow strain rates. The elevated pressures recovered by thermobarometry might lead one to play down the potential for deformation induced dilation in the microstructural development of the mylonites, yet observations on both the matrix mosaics and the veinlets suggest that the opposite is true. High temperatures and slow strain rates would be expected to favour intracrystalline deformation by dislocation creep, yet extremely elongate porphyroclasts appear to represent excised, relatively mildly deformed kink bands or chevron fold limbs.

Mass transfer, whether by diffusion or advection, and brittle deformation, are favoured by the presence of 'water', yet the predominant granulite facies assemblage in these rocks is anhydrous. If a transient hydrous phase existed in these rocks during deformation, what form did it take? One can only speculate on the relative merits of hydrated grain boundaries vs. a free fluid phase. Although the former may suffice to enhance grain boundary diffusion, it would have little effect in brittle fracture, unless the process involved subcritical microcracking (e.g. Atkinson, 1982; den Brok, 1998). If 'water' were present as a fluid, deformation induced grain boundary dilation could provide a mechanism for pumping it through the lower crust.

Brittle failure can be promoted by fast strain rates.

From substructural observations on ultra-fine grains (< 1 m), White and Jiang (1995) have suggested that the Striding–Athabasca mylonites may have supported differential stresses in excess of 150 MPa and experienced strain rates greater than 10^{-11} s^{-1}. However, the present study suggests that the microstructure of the matrix mosaics is indicative of relatively slow strain rates. The apparent contradiction is readily resolved if fast strain rates represent transient events, perhaps leading to the enhancement of brittle failure, and the cataclastic microstructures and fracturing described herein.

The principal conclusion of this study is that it is unwise to seek to identify high-temperature shear zones and to analyse their constituent mylonites by direct analogy with their greenschist facies equivalents. What is a static and post-kinematic microstructure for the one, may be a dynamic microstructure for the other. In particular, it is essential to relate microstructural development in granulite facies mylonites to the metamorphic reactions accompanying the deformation, and to evaluate the potential for positive feedback between the structural and metamorphic processes.

5. Conclusions

Comparison with the microstructure of naturally deformed high-temperature rocks, and experimentally deformed monomineralic and analogue materials, provides insight into the panoply of deformation processes that operated at granulite facies in the Striding–Athabasca mylonite zone, in addition to intracrystalline deformation by dislocation creep. (i) Extensive mass transfer was apparently contemporaneous with brittle fracture and cataclasis. (ii) Reticular microstructure, bimodal grain-size distribution, and extreme phase dispersal in polymineralic matrix mosaics are collectively indicative of efficient grain-scale and aggregate-scale mass transfer, and grain boundary mobility. Orientation families may also indicate grain mobility. (iii) The foregoing processes may have been enhanced by, or may have required, the transient presence of a hydrous phase. (iv) Extreme phase dispersal in granoblastic mosaics, associated with metamorphic reactions requiring positive volume change, would be facilitated by dynamic void creation in the deforming matrix mosaic. Accordingly, the apparently annealed microstructure would be synkinematic. (v) Elongate monocrystalline orthopyroxenes appear to be fragments of dismembered, kinked parent grains, rather than stretched porphyroclasts. (vii) The microstructural evidence for brittle deformation and extensive mass transfer in the granulite facies Striding–Athabasca mylonites highlights the essential role of transient 'water', even in nominally dry rocks. (viii) Because the relative roles of deformation mechanisms and processes are not the same, granulite facies mylonites should not be treated as direct analogues of greenschist facies mylonites.

Acknowledgements

I am particularly indebted to Mike Williams for detailed, constructive criticism and encouragement during the preparation of this paper. I thank Olga Ijewliew and Dave Walker for assistance with the probe analyses and SEM imaging, respectively, and Win Means, Steve Lucas, Ron Vernon, and the Journal reviewers for comments which served to improve the manuscript. This is Geological Survey of Canada contribution 1997-067.

References

Atkinson, B.K., 1982. Subcritical crack propagation in rocks: theory, experimental results and applications. Journal of Structural Geology 4, 41–56.

Basu, A.R., 1977. Textures, microstructures and deformation of ultramafic xenoliths from San Quintin, Baja California. Tectonophysics 43, 213–246.

Beeman, M.L., Kohlstedt, D.L., 1993. Deformation of fine-grained aggregates of olivine plus melt at high temperatures and pressures. Journal of Geophysical Research 98, 6443–6452.

Behrmann, J.H., Mainprice, D., 1987. Deformation mechanisms in a high-temperature quartz–feldspar mylonite: evidence for superplastic flow in the lower continental crust. Tectonophysics 140, 297–305.

Bell, T.H., Etheridge, M.A., 1973. Microstructures of mylonites and their descriptive terminology. Lithos 6, 337–348.

Bell, T.H., Johnson, S.E., 1989. The role of deformation partitioning in the deformation and recrystallisation of plagioclase and K-feldspar in the Woodroffe Thrust mylanite zone, central Australia. Journal of Metamorphic Geology 7, 151–168.

Boland, J.N., Tullis, T.E., 1986. Deformation behaviour of wet and dry clinopyroxenite in the brittle to ductile transition region. In: Hobbs, B.E., Heard, H.C. (Eds.), Mineral and rock deformation: Laboratory studies, American Geophysical Union Monograph, 36, pp. 35–49.

Bons, P.D., Urai, J.L., 1992. Syndeformational grain growth: microstructures and kinetics. Journal of Structural Geology 14, 1101–1109.

Bouchez, J.L., 1977. Plastic deformation of quartzites at low temperatures in an area of natural strain gradient. Tectonophysics 39, 25–50.

Boullier, A.M., Bouchez, J.L., 1978. Le quartz en rubans dans les mylonites. Bulletin de la Societé géologique de France 7, 253–262.

Boullier, A.M., Gueguen, Y., 1975. SP-Mylonites: the origin of some mylonites by superplastic flow. Contributions to Mineralogy and Petrology 50, 93–104.

Brodie, K.H., 1981. Variation in amphibole and plagioclase composition with deformation. Tectonophysics 78, 385–402.

Brodie, K.H., 1995. The development of oriented symplectites during deformation. Journal of metamorphic Geology 13, 499–508.

Brunel, M., 1980. Quartz fabrics in shear-zone mylonite: evidence for a major imprint due to late strain increments. Tectonophysics 64, T33–T44.

Carney, J.N., Treloar, P.J., Barton, C.M., Crow, M.J., Evans, J.A., Simango, S., 1991. Deep-crustal granulites with migmatitic and mylonitic fabrics from the Zambesi Belt, northeastern Zimbabwe. Journal of metamorphic Geology 9, 461–479.

Carter, N.L., Raleigh, C.B., 1969. Principal stress directions from plastic flow in crystals. Geological Society of America Bulletin 80, 1231–1264.

Cobbold, P.R., Cosgrove, J.W., Summers, J.M., 1971. Development of internal structures in deformed anisotropic rocks. Tectonophysics 12, 23–53.

Darot, M., Boudier, F., 1975. Mineral lineations in deformed peridotites: kinematic meaning. Pétrologie 1, 225–236.

den Brok, B., Kruhl, J.H., 1996. Ductility of garnet as an indicator of extremely high temperature deformation: Discussion. Journal of Structural Geology 18, 1369–1373.

den Brok, S.W.J., 1998. Effect of microcracking on pressure-solution strain rate: The Gratz grain-boundary model. Geology 26, 915–918.

Drury, M.R., Humphreys, F.J., 1988. Microstructural shear criteria associated with grain-boundary sliding during ductile deformation. Journal of Structural Geology 10, 83–89.

Elliot, D., 1973. Diffusion flow laws in metamorphic rocks. Geological Society of America Bulletin 84, 2645–2664.

Etchecopar, A., Vasseur, G., 1987. A 3-D kinematic model of fabric development in polycrystalline aggregates: comparisons with experimental and natural examples. Journal of Structural Geology 9, 705–717.

Etheridge, M.A., 1975. Deformation and recrystallisation of orthopyroxene from the Giles Complex, central Australia. Tectonophysics 25, 87–114.

Etheridge, M.A., 1983. Differential stress magnitudes during regional deformation and metamorphism; Upper bound imposed by tensile fracturing. Geology 11, 231–234.

Etheridge, M.A., Wall, V.J., Cox, S.F., Vernon, R.H., 1984. High fluid pressures during regional metamorphism and deformation: Implications for mass transport and deformation mechanisms. Journal of Geophysical Research 89, 4344–4358.

Etheridge, M.A., Wall, V.J., Vernon, R.H., 1983. The role of the fluid phase during regional metamorphism and deformation. Journal of metamorphic Geology 1, 205–226.

Farver, J.R., Yund, R.A., 1995. Grain boundary diffusion of oxygen, potassium and calcium in natural and hot-pressed aggregates. Contributions to Mineralogy and Petrology 118, 340–355.

Farver, J.R., Yund, R.A., 1996. Volume and grain boundary diffusion of calcium in natural and hot-pressed calcite aggregates. Contributions to Mineralogy and Petrology 123, 77–91.

Fitz Gerald, J.D., Stunitz, H., 1993. Deformation of granitoids at low metamorphic grade. I: Reactions and grain size reduction. Tectonophysics 221, 269–297.

Flinn, D., 1969. Grain contacts in crystalline rocks. Lithos 3, 361–370.

Florence, F.P., Spear, F.S., 1995. Intergranular diffusion kinematics of Fe and Mg during retrograde metamorphism of a pelitic gneiss from the Adirondack Mountains. Earth and Planetary Science Letters 134, 329–340.

Gapais, D., Barbarin, B., 1986. Quartz fabric transition in a cooling syntectonic granite (Hermitage Massif, France). Tectonophysics 125, 357–370.

Goode, A.D.T., 1978. High temperature, high strain rate deformation in the lower crustal Kalka Intrusion, Central Australia. Contributions to Mineralogy and Petrology 66, 137–148.

Gregg, W., 1978. The production of tabular grain shapes in metamorphic rocks. Tectonophysics 49, T19–T24.

Gueguen, Y., Boullier, A.M., 1974. Evidence of superplasticity in mantle peridotites. In: Strens, R.G.J. (Ed.), The Physics and Chemistry of Minerals and Rocks, pp. 20–33.

Hanmer, S., 1982. Microstructure and geochemistry of plagioclase and microcline in naturally deformed granite. Journal of Structural Geology 4, 197–213.

Hanmer, S., 1984. Strain-insensitive foliations in polymineralic rocks. Canadian Journal of Earth Sciences 21, 1410–1414.

Hanmer, S., 1987. Textural map-units in quartzofeldspathic mylonitic rocks. Canadian Journal of Earth Sciences 24, 2065–2073.

Hanmer, S., 1988. Ductile thrusting at mid-crustal level, southwestern Grenville Province. Canadian Journal of Earth Sciences 25, 1049–1059.

Hanmer, S., 1994. Geology, East Athabasca mylonite triangle, Stony Rapids area, northern Saskatchewan, Geological Survey of Canada Map 1859A. Geological Survey of Canada Map, scale 1:100 000.

Hanmer, S., 1997. Geology of the Striding–Athabasca mylonite zone, northern Saskatchewan and southeast District of Mackenzie. Geological Survey of Canada Bulletin 501, 92.

Hanmer, S., McEachern, S.J., 1992. Kinematical and rheological evolution of a crustal-scale ductile thrust zone, Central Metasedimentary Belt, Grenville orogen. Canadian Journal of Earth Sciences 29, 1779–1790.

Hanmer, S., Parrish, R., Williams, M., Kopf, C., 1994. Striding–Athabasca mylonite zone: Complex Archean deep-crustal deformation in the East Athabasca mylonite triangle, N. Saskatchewan. Canadian Journal of Earth Sciences 31, 1287–1300.

Hanmer, S., Williams, M., Kopf, C., 1995a. Striding–Athabasca mylonite zone: Implications for Archean and Early Proterozoic tectonics of the western Canadian Shield. Canadian Journal of Earth Science 32, 178–196.

Hanmer, S., Williams, M., Kopf, C., 1995b. Modest movements, spectacular fabrics in an intracontinental deep-crustal strike-slip fault: Striding–Athabasca mylonite zone, NW Canadian Shield. Journal of Structural Geology 17, 493–507.

Herwegh, M., Handy, M.R., 1996. The evolution of high-temperature mylonitic microfabrics: evidence from simple shearing of a quartz analogue (norcamphor). Journal of Structural Geology 18, 689–710.

Hickey, K.A., Bell, T.H., 1996. Syn-deformational grain growth: matrix coarsening during foliation development and regional metamorphism rather than by static annealing. European Journal of Mineralogy 8, 1351–1373.

Hirth, G., Tullis, J., 1992. Dislocation creep regimes in quartz aggregates. Journal of Structural Geology 14, 145–159.

Ji, S., Mainprice, D., 1988. Natural deformation fabrics of plagioclase: implications for slip systems and seismic anisotropy. Tectonophysics 147, 145–163.

Ji, S., Mainprice, D., Boudier, F., 1988. Sense of shear in high-temperature movement zones from the fabric asymmetry of plagioclase feldspars. Journal of Structural Geology 10, 73–81.

Ji, S., Martignole, J., 1994. Ductility of garnet as an indicator of extremely high temperature deformation. Journal of Structural Geology 16, 985–996.

Ji, S., Salisbury, M., Hanmer, S., 1993. Petrofabric, P-wave anisotropy and seismic reflectivity of high-grade tectonites. Tectonophysics 222, 195–226.

Kerrich, R., Allison, I., Barnett, R.L., Moss, S., Starkey, J., 1980. Microstructural and chemical transformations accompanying deformation of for stress corrosion cracking and superplastic flow. Contributions to Mineralogy and Petrology 73242, 221–242.

Knipe, R.J., 1989. Deformation mechanisms—recognition from natural tectonites. Journal of Structural Geology 11, 127–146.

Knipe, R.J., Law, R.D., 1987. The influence of crystallographic orientation and grain boundary migration on microstructural and textural evolution in an *S–C* mylonite. Tectonophysics 135, 155–169.

Kohlstedt, D.L., Vander Sande, J.B., 1973. Transmission electron microscopy investigation of the defect microstructure of four

natural orthopyroxenes. Contributions to Mineralogy and Petrology 42, 169–180.

Kohlstedt, D.L., Weathers, M.S., 1980. Deformation-induced microstructures, paleopiezometers, and differential stresses in deeply eroded fault zones. Journal of Geophysical Research 85, 6269–6285.

Kruse, R., Stunitz, H., 1999. Deformation mechanisms and phase distribution in mafic high-temperature mylonites from the Jotun Nappe, southern Norway. Tectonophysics 303, 223–250.

Lafrance, B., John, B.E., Scoates, J.S., 1996. Syn-emplacement recrystallisation and deformation microstructures in the Poe Mountain anorthosite, Wyoming. Contributions to Mineralogy and Petrology 122, 431–440.

Lafrance, B., Vernon, R.H., 1993. Mass transfer and microfracturing in gabbroic mylonites of the Guadalupe igneous complex, California. In: Boland, J.N., Fitz Gerald, J.D. (Eds.), Defects and Processes in the Solid State: Geoscience Applications. The McLaren Volume, pp. 151–167.

Lister, G.S., Dornsiepen, U.F., 1982. Fabric transitions in the Saxony granulite terrain. Journal of Structural Geology 4, 81–92.

Lister, G.S., Snoke, A.W., 1984. *S–C* Mylonites. Journal of Structural Geology 6, 617–638.

MacKenzie, D.B., 1960. High-temperature alpine-type peridotite from Venezuela. Geological Society of America Bulletin 71, 303–318.

Mackinnon, P., Fueten, F., Robin, P.Y., 1997. A fracture model for quartz ribbons in straight gneisses. Journal of Structural Geology 19, 1–14.

Mawer, C.K., Fitz Gerald, J.D., 1993. Microstructure of kink band boundaries in naturally deformed Chewings Range Quartzite. In: Boland, J.N., Fitz Gerald, J.D. (Eds.), Defects and Processes in the Solid State: Geoscience Applications. The McLaren Volume, pp. 49–84.

Means, W.D., 1981. The concept of steady-state foliation. Tectonophysics 78, 179–199.

Means, W.D., 1983. Microstructure and micromotion in recrystallized flow of octachloropropane: a first look. Geologische Rundschau 72, 511–528.

Means, W.D., 1989. Synkinematic microscopy of transparent polycrystals. Journal of Structural Geology 11, 163–174.

Means, W.D., Dong, H.G., 1982. Some unexpected effects of recrystallisation on the microstructure of materials deformed at high temperature. Mitteilungen Geologische Institut ETH Neue Folge 239A, 205–207.

Means, W.D., Park, Y., 1994. New experimental approach to understanding igneous texture. Geology 22, 323–326.

Mercier, J.C., 1985. Olivine and pyroxenes. In: Wenk, H.R. (Ed.), Preferred Orientation in Deformed Metals and Rocks: An Introduction to Modern Texture Analysis, pp. 407–430.

Mercier, J.C., Nicolas, A., 1975. Textures and fabrics of upper-mantle peridotites as illustrated by xenoliths from basalts. Journal of Petrology 16, 454–487.

Nazé, L., Doukhan, N., Doukhan, J.C., Latrous, K., 1987. A TEM study of lattice defects in naturally ands experimentally deformed orthopyroxenes. Bulletin de Minéralogie 110, 497–512.

Newman, J., Lamb, W.M., Vissers, R.L.M., 1999. Deformation processes in a peridotite shear zone: reaction-softening by an H_2O-deficient, continuous net transfer reaction. Tectonophysics 303, 193–222.

Nicolas, A., Boudier, F., Boullier, A.M., 1973. Mechanisms of flow in naturally and experimentally deformed peridotites. American Journal of Science 273, 853–876.

Nicolas, A., Poirier, J.P., 1976. Crystalline plasticity and solid state flow in metamorphic rocks. Wiley, New York.

Nyman, M.W., Tracy, R.J., 1993. Petrological evolution of amphibolite shear zones, Cheyenne Belt, south-eastern Wyoming, USA. Journal of metamorphic Geology 11, 757–773.

Olesen, N.O., 1987. Plagioclase fabric developement in a high-grade shear zone, Jotunheimen, Norway. Tectonophysics 142, 291–308.

Park, Y., Means, W.D., 1996. Direct observation of deformation processes in crystal mushes. Journal of Structural Geology 18, 847–858.

Passchier, C.W., Simpson, C., 1986. Porphyroclast systems as kinematic indicators. Journal of Structural Geology 8, 831–844.

Ramsay, J.G., 1967. Folding and Fracturing of Rocks. McGraw Hill, New York.

Ross, J.V., Mercier, J.C., Ave Lallemant, H.G., Carter, N.L., Zimmerman, J., 1980. The Vourinos ophiolite complex, Greece: the tectonite suite. Tectonophysics 70, 63–83.

Ross, J.V., Wilks, K.R., 1995. Effects of a third phase on the mechanical and microstructural evolution of a granulite. Tectonophysics 241, 303–315.

Rutter, E.H., Brodie, K.H., 1988. Experimental approaches to the study of deformation/metamorphism relationships. Mineralogical Magazine 52, 35–42.

Rutter, E.H., Brodie, K.H., 1992. Rheology of the lower crust. In: Fountain, D.M., Arculus, R.J., Kay, R.W. (Eds.), Continental Lower Crust, pp. 201–267.

Snoeyenbos, D.R., Williams, M.L., Hanmer, S., 1995. An Archean eclogite facies terrane in the western Canadian Shield. European Journal of Mineralogy 7, 1251–1272.

Stel, H., 1981. Crystal growth in cataclasites: diagnostic microstructures and implications. Tectonophysics 78, 585–600.

Stunitz, H., 1998. Syndeformational recrystallization—dynamic or compositionally induced? Contributions to Minerology and Petrology 131, 219–236.

Tubia, J.M., 1994. The Ronda peridotites (Los Reales nappe): an example of the relationship between lithospheric thickening by oblique tectonics and late extensional deformation within the Betic Cordillera (Spain). Tectonophysics 238, 381–398.

Tullis, J., 1990. Experimental studies of deformation mechanisms and microstructures in quartzo-feldspathic rocks. In: Barber, D.J., Meredith, P.G. (Eds.), Deformation Processes in Minerals, Ceramics and Rocks, pp. 190–227.

Tullis, J., Yund, R.A., 1991. Diffusion creep in feldspar aggregates: experimental evidence. Journal of Structural Geology 13, 987–1000.

Tullis, J., Yund, R.A., 1992. The brittle–ductile transition in feldspar aggregates: an experimental study. In: Evans, B., Wong, T.F. (Eds.), Fault mechanics and transport properties of rocks: a festschrift in honor of W.F. Brace, pp. 89–117.

Urai, J.L., 1983. Water assisted dynamic recrystallisation and weakening in polycrystalline bischofite. Tectonophysics 96, 125–157.

Urai, J.L., Means, W.D., Lister, G.S., 1986. Dynamic recrystallization of minerals. In: Hobbs, B.E., Heard, H.C. (Eds.), Mineral and rock deformation: Laboratory studies, American Geophysical Union Monograph. Geophysical Monograph, pp. 161–200.

Vernon, R.H., 1974. Metamorphic Processes, Reactions and Microstructure Development. Allen & Unwin, London.

Weathers, M.S., Bird, J.M., Cooper, R.F., Kohlstedt, D.L., 1979. Differential stress determined from deformation-induced microstructures of the Moine Thrust Zone. Journal of Geophysical Research 84, 7495–7509.

White, J.C., Jiang, D., 1995. Strength regimes in the lower crust: implications for crustal architecture, with reference to the Snowbird Tectonic Zone. Lithoprobe, Trans-Hudson Orogen Transect Report 48, 219–224.

White, J.C., Mawer, C.K., 1986. Extreme ductility of feldspars from a mylonite, Parry Sound, Canada. Journal of Structural Geology 8, 133–143.

White, J.C., Mawer, C.K., 1988. Dynamic recrystallisation and associated exsolution in perthites: evidence of deep crustal thrusting. Journal of Geophysical Research 93, 325–337.

White, S.H., 1976. The effects of strain on microstructures, fabrics

and deformation mechanisms in quartzites. Philosophical Transactions of the Royal Society, London A283, 69–86.

White, S.H., Burrows, S.E., Carreras, J., Shaw, N.D., Humphreys, F.J., 1980. On mylonites in ductile shear zones. Journal of Structural Geology 2, 175–187.

Williams, M.L., Melis, E.A., Kopf, C., Hanmer, S., 1999. Microstructural tectonometamorphic processes and granulite facies gneissic layering; a mechanism for high-temperature metamorphic segregation. Journal of metamorphic Geology (in press).

Williams, P.F., Compagnoni, R., 1983. Deformation and metamorphism in the Bard area of the Sesia Lanzo Zone, Western Alps, during subduction and uplift. Journal of metamorphic Geology 1, 117–140.

Wilson, C.J.L., 1986. Deformation induced recrystallisation of ice: the application of in situ experiments. In: Hobbs, B.E., Heard, H.C. (Eds.), Mineral and rock deformation: Laboratory studies, American Geophysical Union Monograph. Geophysical Monograph, 36, pp. 213–232.

Yund, R.A., 1997. Rates of grain boundary diffusion through enstatite and forsterite reaction rims. Contributions to Mineralogy and Petrology 126, 224–236.

Yund, R.A., Quigley, J., Tullis, J., 1989. The effect of dislocations on bulk diffusion in feldspars during metamorphism. Journal of metamorphic Geology 7, 337–341.

Yund, R.A., Smith, B.M., Tullis, J., 1981. Dislocation-assisted diffusion of oxygen in albite. Physics and Chemistry of Minerals 7, 185–189.

Yund, R.A., Tullis, J., 1980. The effect of water, pressure and strain on Al/Si order–disorder kinetics in feldspar. Contributions to Mineralogy and Petrology 72, 297–302.

Zhang, Y., Hobbs, B.E., Jessell, M.W., 1994a. The effect of grain-boundary sliding on fabric development in polycrystalline aggregates. Journal of Structural Geology 16, 1315–1325.

Zhang, Y., Hobbs, B.E., Ord, A., 1994b. A numerical simulation of fabric development in polycrystalline aggregates with one slip system. Journal of Structural Geology 16, 1297–1313.